Journal of Crystal Growth 425 (2015) 274–278

Contents lists available at ScienceDirect

Journal of Crystal Growth

journal homepage: www.elsevier.com/locate/jcrysgro

The impact of substrate selection for the controlled growth of graphene by molecular beam epitaxy

T. Schumann, J.M.J. Lopes *, J.M. Wofford, M.H. Oliveira Jr.[1], M. Dubslaff, M. Hanke, U. Jahn, L. Geelhaar, H. Riechert

Paul-Drude-Institut für Festkörperelektronik, Hausvogteiplatz 5–7, 10117 Berlin, Germany

ARTICLE INFO

Communicated by A. Brown
Available online 24 February 2015

Keywords:
A1. Surfaces
A1. X-ray diffraction
A3. Molecular beam epitaxy
B1. Nanomaterials

ABSTRACT

We examine how substrate selection impacts the resulting film properties in graphene growth by molecular beam epitaxy (MBE). Graphene growth on metallic as well as dielectric templates was investigated. We find that MBE offers control over the number of atomic graphene layers regardless of the substrate used. High structural quality could be achieved for graphene prepared on Ni (111) films which were epitaxially grown on MgO (111). For growth either on Al_2O_3 (0001) or on $(6\sqrt{3}\times 6\sqrt{3})R30^\circ$-reconstructed SiC (0001) surfaces, graphene with a higher density of defects is obtained. Interestingly, despite their defective nature, the layers possess a well defined epitaxial relation to the underlying substrate. These results demonstrate the feasibility of MBE as a technique for realizing the scalable synthesis of this two-dimensional crystal on a variety of substrates.

1. Introduction

Graphene, a single layer of carbon atoms arranged in a two-dimensional hexagonal lattice, is widely regarded as a revolutionary material, due primarily to its electronic properties [1–3]. The high charge carrier mobility and the ambipolar field effect measured in graphene are particularly appealing for electronic device applications [4]. Furthermore, it is known that ordered stacks of multiple graphene layers (e.g. bi- or trilayer graphene) also possess intriguing features, such as an electric field and stacking-order-dependent band structure [5–7]. These phenomena are not observed in monolayer graphene and open yet more exciting possibilities, such as the realization of devices with a gate-tunable band gap [7,8].

Hence, in terms of synthesis, a consensus has formed that the growth of high-quality, large-scale graphene films with precise control over the number of atomic layers is critical since it will enable applications where not only mono-, but also few-layer thick films will be required [9]. Although techniques such as SiC surface graphitization [10–12] and chemical vapor deposition (CVD) on Cu [13,14] have proved to be suitable for large-area synthesis, both have inherent drawbacks. The former method is restricted to a single substrate material (which happens currently to be costly). In addition, the controlled growth of a specific number of graphene layers on SiC with complete thickness homogeneity remains challenging. CVD on Cu produces continuous graphene films which are exclusively one monolayer thick, since the precursor molecules are efficiently cracked only at the original, exposed metal surface. Similar to graphene growth on SiC, despite intensive ongoing research, the controlled formation of uniform few-layer graphene on Cu remains to be demonstrated. In this context, molecular beam epitaxy (MBE) appears to be a promising alternative. MBE is one of the most prominent techniques for the production of high-quality, single-crystal semiconductor films and multilayer heterostructures [15]. MBE typically does not involve catalytic surface processes, and thus holds promise for the growth of one to ~few graphene layers on a wider variety of substrates, including insulators and semiconductors. Exact deposition rates and sub-monolayer thickness control are additional significant advantages offered by MBE which will be required to achieve well-controlled, layer-by-layer graphene growth.

Although it is a relatively new topic of study within the MBE community, there have been several attempts to prepare graphene by employing this method. Previously examined templates include Si [16,17], SiO_2 [18], SiC [19], Al_2O_3 [17,20–22], Ni [23,24], and mica [18,25]. The various substrates and growth conditions used during synthesis resulted in carbon materials with different structural quality and morphology, ranging from highly disordered sp^2-bonded carbon [16–18] or nanocrystalline (defective) graphene layers [17,20–22], to state-of-the-art quality graphene (either continuous layers [24] or isolated islands [25]). In spite of the apparent discrepancy between results, the collection of existing studies nevertheless already point to the fact that MBE is indeed a

* Corresponding author.
E-mail address: lopes@pdi-berlin.de (J.M.J. Lopes).
[1] Permanent address: Departamento de Física, ICEx, Universidade Federal de Minas Gerais-UFMG, C.P. 702, 31270-901, Belo Horizonte, MG, Brazil.

http://dx.doi.org/10.1016/j.jcrysgro.2015.02.060
0022-0248/

promising technique for achieving the controlled growth of graphene over large areas. In addition, from a fundamental point of view, MBE is an ideal tool for generating a detailed understanding of nucleation and growth mechanisms due to its compatibility with in situ characterization. This is especially important as graphene growth has developed into a rich research field in its own right. It has already been shown to differ from conventional thin-film epitaxy in significant ways, following mechanisms such as van der Waals epitaxy and growth from below [18,21,24,25]. In this context, it is important to mention other studies regarding graphene growth in UHV (by both physical vapor deposition [PVD] and CVD) which have closely replicated MBE growth conditions. In particular, surface scientists have carefully examined graphene formation on metals such as Ru, Ir, Cu and Au, often using powerful in situ characterization techniques such as low-energy electron microscopy (LEEM). These studies have revealed a rich, complex array of growth phenomena [26–31]. This body of literature – of which the cited references are only a few examples – may not be MBE growth in the strictest terms, but does serve to illustrate the utility of a well-controlled, the UHV growth method in the study of graphene synthesis.

In this contribution we report research aimed at the controlled preparation of graphene layers by MBE. We focus specifically on how the choice of substrate impacts the properties of the resulting graphene film by comparing and contrasting results obtained for growth on three very different surfaces as illustrative examples: Ni (111) films which were epitaxially grown on MgO (111), Al_2O_3 (0001), and SiC (0001) (offering a $(6\sqrt{3}\times 6\sqrt{3})R30^\circ$ C-rich surface reconstruction). These results demonstrate the potential of MBE for the realization of the controlled epitaxial growth of graphene films (mono- to few-layer thick) with substrate flexibility.

2. Experimental

Graphene growth was performed in a dedicated MBE system with a base pressure of 1×10^{-10} mbar. The system is equipped with a solid carbon source composed of a resistively heated highly oriented pyrolytic graphite (HOPG) filament that operates nominally between 2200 and 2400 °C. In this temperature range the carbon flux is $\sim 6\times 10^{12}$ atoms/cm^2 s. All substrates [the Ni/MgO (111) and SiC (0001) were sized 1 cm^2, and Al_2O_3 (0001) were full two-inch wafers] were degassed in a preparation chamber at 350 °C for 30 min before transfer to the growth chamber. Note that all substrates employed a 1 μm thick Ti film (deposited *ex situ* by RF-sputtering) on the backside to allow non-contact radiative heating. In the case of Ni/MgO (111), 150 nm thick epitaxial Ni (111) films were grown on MgO (111) in the same MBE cluster prior to carbon deposition. The 2.490 Å in-plane lattice parameter of the (111) Ni surface closely matches that of graphene. More details about the synthesis of the Ni (111) films can be found elsewhere [24]. For the SiC (0001) substrates, the surface preparation which allows for the creation of a $(6\sqrt{3}\times 6\sqrt{3})R30^\circ$ reconstruction (referred to as $6\sqrt{3}$, for simplicity) is performed *ex situ* at high temperatures (~1450 °C) in a RF-furnace prior to introducing the sample to the MBE cluster. The thermal annealing procedures utilized for this can be found in Ref. [32]. The MBE growth of graphene was performed using different growth temperatures and times. The temperature chosen for graphene growth on Ni/MgO (111) was 765 °C, with deposition time ranging from 40 to 200 min. For Al_2O_3 (0001) and $6\sqrt{3}$-SiC (0001) growth temperatures ranging from 900 to 1000 °C were employed, with a growth time of 240 min. The structural properties of the grown films were investigated by Raman spectroscopy. The spectra shown in the next section, which were acquired with a spatial resolution of 1 μm and excitation wavelength of 482 nm, are representative of large-area growth by MBE. Analyses of different surface regions yielded similar results. In addition, scanning electron microscopy (SEM) and grazing-incidence X-ray diffraction (GID) were used to investigate the surface morphology and structure of the samples, respectively.

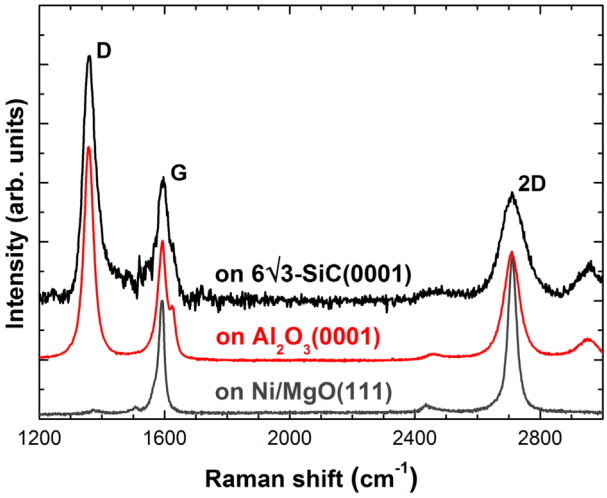

Fig. 1. Raman spectra of MBE grown graphene films on Ni/MgO (111) (gray), Al_2O_3 (0001) (red), and reconstructed $6\sqrt{3}$-SiC (0001) substrates (black). The film grown on Ni/MgO (111) was deposited at a substrate temperature of 765 °C over 120 min (average thickness of 2 MLs) while those on Al_2O_3 and SiC were grown at 900 °C and deposition times of 240 min (average thickness of 1.5 MLs). The intensity is normalized with respect to the G peak, the spectra are offset for visibility, and the substrate related background signal is subtracted from the spectrum recorded on SiC. (For interpretation of the references to color in this figure legend, the reader is referred to the web version of this article.)

3. Results and discussions

Raman spectroscopy, which is a commonly accepted proxy for the crystalline quality of graphene [33,34], was used to examine the resulting films. Representative spectra are shown in Fig. 1 for graphene grown on each substrate examined here, with each displaying the characteristic peaks of sp^2-bonded carbon. The appearance of well-defined and intense G and 2D peaks is clear evidence for the formation of graphene. In the case of graphene grown on Ni/MgO (111) (gray spectrum), the negligible intensity of the D peak indicates that extremely few structural defects, such as point vacancies or rotational grain boundaries, are present in the film. This is corroborated by the narrow widths (full widths at half maxima–FWHM) of the G and 2D peaks, $w_G=17$ cm^{-1} and $w_{2D}=32$ cm^{-1}, which show the presence of a well-ordered crystal structure with a degree of perfection similar to that observed in exfoliated graphene flakes [33,34] and CVD-prepared layers [14]. The high crystalline quality of the graphene is consistent with its relatively low nucleation density on Ni/MgO (111) substrates (Fig. 4a), which is facilitated by significant carbon adatom diffusion on the metallic surface. This leads to a correspondingly low line-density of grain boundaries, regardless of the crystallographic orientation of the individual domains.

Raman spectra from graphene grown on Al_2O_3 (Fig. 1, red) and $6\sqrt{3}$-SiC (black) both reveal similar features. The intense defect-related D peaks but well-defined and symmetric G and 2D peaks in spectra from films grown on both dielectric substrates are characteristic of defective graphene [34,35]. The peak intensity ratios I_D/I_G are comparable for both samples (1.9 for Al_2O_3 and 2.1 for $6\sqrt{3}$-SiC). However, the FWHM of the peaks are considerably lower in case for growth on Al_2O_3 ($w_D=34$ cm^{-1}, $w_G=32$ cm^{-1}, and $w_{2D}=56$ cm^{-1}) when compared with graphene synthesized on the $6\sqrt{3}$-SiC ($w_D=43$ cm^{-1}, $w_G=42$ cm^{-1}, and $w_{2D}=75$ cm^{-1}). Empirical

estimates yield lateral domain sizes of few tens of nanometer in both cases [21,32].

This Raman analysis suggests that growth on Al_2O_3 (0001) yields graphene with a slightly higher structural quality than $6\sqrt{3}$-SiC (0001). These two substrates were chosen to investigate graphene growth directly on insulating surfaces because – in addition to the high growth temperatures their excellent thermal stability allows – their hexagonal surface symmetry may be conducive to graphene epitaxy. The $6\sqrt{3}$-SiC (0001) surface is a carbon rich reconstruction of the Si-face of hexagonal SiC. It is isomorphic to graphene, i.e. it possesses the same honeycomb carbon lattice structure and a similar lattice parameter as graphene [36,37] (note, however, it has about 30% of its atoms covalently bound to the SiC substrate [38]). Therefore, due to its similarities to graphene, such a surface can be employed as a template to investigate the quasi-homoepitaxial growth of graphene. Al_2O_3 (0001), on the other hand, has a hexagonal surface symmetry with a lattice parameter (4.750 Å) approximately twice that of graphene (2.461 Å) [39], making growth on this substrate heteroepitaxial. Thus, perhaps paradoxically, heteroepitaxy is more conducive to the formation of high-quality graphene (fewer defects/less disorder) in this instance than quasi-homoepitaxial growth. A possible explanation for the lower quality of graphene resulting from growth on $6\sqrt{3}$-SiC (0001) and Al_2O_3 (0001) (in comparison to films obtained on Ni/MgO (111) substrates) is an absence of epitaxial ordering with respect to the substrate. The formation of small, defective graphene crystals with random crystallographic orientations – which is usually not observed for graphene grown on metals [24,26,31] – would represent a fundamental obstacle to the growth of high-quality material on insulators. However, if the graphene nanocrystals are epitaxially aligned with the substrate they can coalesce into a single domain. Strict epitaxy may thus be a prerequisite for high-quality growth on dielectrics.

In order to investigate this aspect of graphene growth on these substrates we have conducted grazing incidence diffraction (GID) at beamline ID10 at the European Synchrotron Radiation Facility (ESRF) in Grenoble using an X-ray energy of 10 keV. This highly surface sensitive technique provides the possibility of not only measuring the lattice parameters of two-dimensional films with extraordinary precision, but also of gaining information about the in-plane relation of the films and their respective substrates. Fig. 2 presents line-scans over the graphene G (10–10) reflection in the radial direction (i.e. probing the distance of the lattice planes). For easier interpretation, the *x*-axis is scaled to represent the lattice parameter of graphene. The reflection obtained from graphene on

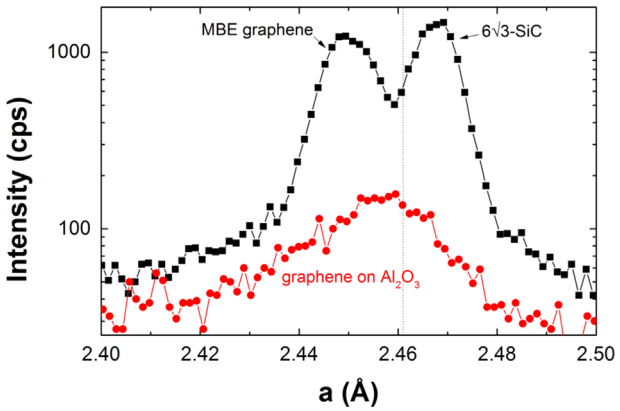

Fig. 2. Radial line scans of the graphene (10–10) reflections (transformed to real space) recorded from graphene films grown on the $6\sqrt{3}$-SiC (0001) and on Al_2O_3 (0001). The *x*-axis is scaled to represent the lattice parameter of graphene, the dotted line marks the lattice parameter of relaxed graphite.

$6\sqrt{3}$-SiC (0001) shows a doublet structure with two peaks centered at 2.450 Å and 2.468 Å. The latter one can be assigned to the underlying C-rich reconstruction, as confirmed by reference measurements on a bare substrate. The peak at 2.450 Å therefore corresponds to the grown graphene, which means that the film possesses a lattice parameter ~0.45% smaller than that of relaxed graphite (2.461 Å) [39]. This shrinkage can be explained by the presence of point defects [32]. The scan recorded from the film on Al_2O_3 (0001) consists of a single peak, centered at 2.456 Å. The lattice contraction in comparison to graphite amounts only to ~0.20%, suggesting that the graphene lattice possesses fewer point defects in this case (in agreement with results obtained by Raman spectroscopy). On the other hand, the width of the peak is larger than for the growth on $6\sqrt{3}$-SiC (0001), which means that there is a broader variation in the graphene lattice parameter.

To investigate the in-plane orientation of the graphene films, line scans in the angular direction with an azimuthal range of 130° were performed, and are presented in Fig. 3(a). Only graphene peaks with a separation of 60° emerge, with an intensity that is two orders of magnitude higher than the background signal. Hence, the films possess a single crystallographic orientation with six-fold symmetry, as expected for graphene. Additional measurements (not shown here) reveal that the graphene films possess a single in-plane orientation with their respective substrates, and that this alignment is rotated by an angle of 30° [i.e. Al_2O_3/SiC (11–20) ∥ graphene (1–100)]. Remarkably, such an epitaxial alignment of the layers occurs even though previous results (obtained by X-ray photoelectron spectroscopy) revealed that they only weakly interact with the underlying substrate [21,32]. This indicates that van der Waals forces may play an important role in the process of epitaxial arrangement, although it is not yet possible to state that the whole process is purely based on this type of interaction, as it is expected for ideal van der Waals epitaxy [40]. Fig. 3(b) shows the in-plane alignment of the films with higher resolution. Even though the complete carbon lattice is aligned to the substrate, disorder and slight rotational misalignment between different domains is possible. The graphene grown on the $6\sqrt{3}$-SiC (0001) shows a narrow peak with a FWHM of 0.6°, indicating a strict epitaxial alignment to the substrate. In contrast, the width of the peak recorded from the film grown on Al_2O_3 (0001) amounts to 3.5°. Therefore, a larger degree of rotational disorder is present in the film and the epitaxial relation is less well defined when compared to growth on the quasi-homoepitaxial substrate. Note that the peak intensity for growth on Al_2O_3 is one order of magnitude lower compared with growth on $6\sqrt{3}$-SiC (0001). Nevertheless, since the peak's width in both radial and angular direction is larger, the integrated peak intensities are comparable for both samples, as expected given their similar thicknesses.

At first glance the Raman and GID analyses of graphene growth by MBE on these two substrates offer potentially contradictory results. As can be expected, growing on a (nearly) lattice matched substrate [$6\sqrt{3}$-SiC (0001)] leads to superior in-plane ordering in the graphene films when compared to growth on a heteroepitaxial substrate (Al_2O_3). However, these differences in epitaxial alignment seem not to be manifested in the structural quality, as determined by Raman spectroscopy, which revealed that the films on both substrates have similar characteristics, with even slightly narrower peaks widths obtained for the case of growth on Al_2O_3 (0001). This suggests that the final quality of graphene films is ultimately not limited by defects in grain boundary regions between graphene domains of different orientations, but rather by the presence of point defects. Or, alternatively, that coalescence between neighboring graphene domains does not take place without the incorporation of defects, regardless of the epitaxial relation between them.

In addition to achieving epitaxial growth on different substrates, it is also desirable to exert control over the thickness of graphene films during synthesis. For the three substrates investigated here, the average thickness of the graphene film could easily be modulated with the growth time. This is an important benefit of solid-source MBE in comparison to CVD-based processes. Nevertheless, the existence of local thickness variations related to substrate features such as step edges cannot be excluded. This is particularly challenging during growth on Ni substrates.

We have employed SEM in conjunction with Raman spectroscopy to evaluate the thickness distribution within graphene films grown on Ni/MgO (111) (Fig. 4). We find that a complete monolayer of graphene forms prior to any few-layer regions developing, which is consistent with monolayer graphene bound to the Ni surface being the energetically preferred state [41]. Upon completion of the first monolayer thicker regions of graphene begin to form, and rather than forming an additional continuous layer, they instead often form localized regions of thicker graphene. Despite the fact that the films offer thickness inhomogeneities, their average thickness scales well with deposition time, and indicate a growth rate of 1 monolayer of graphene each 60 min which enables precise, submonolayer thickness control. This growth rate indicates that ~18% of the carbon atoms impinging on the surface become incorporated into the graphene film, as compared to ~7%

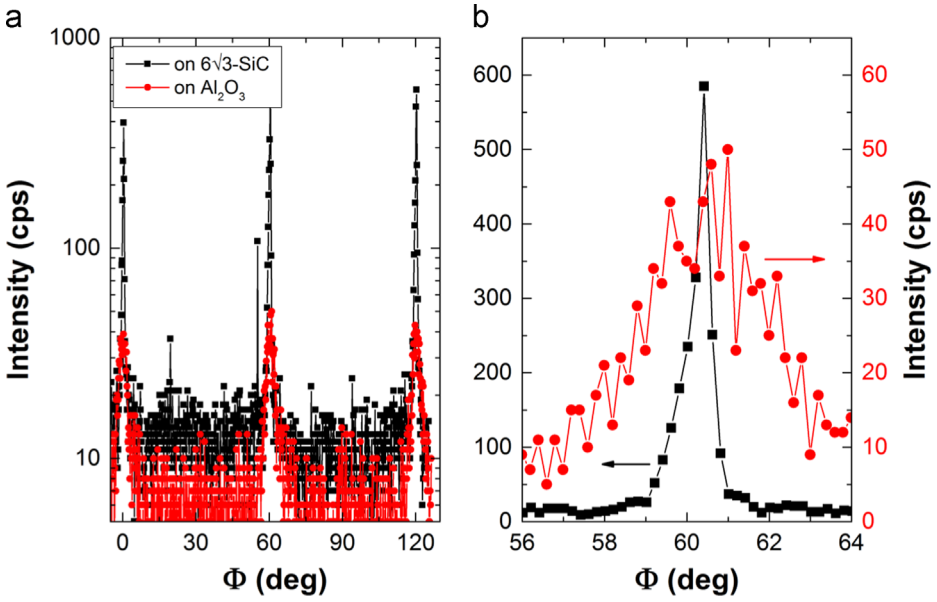

Fig. 3. Scans in the angular direction of the graphene (11–20) reflection [Al_2O_3 (3–300)/SiC(2–200) ∥ graphene (11–20)]. Note the different scales in (a) and (b).

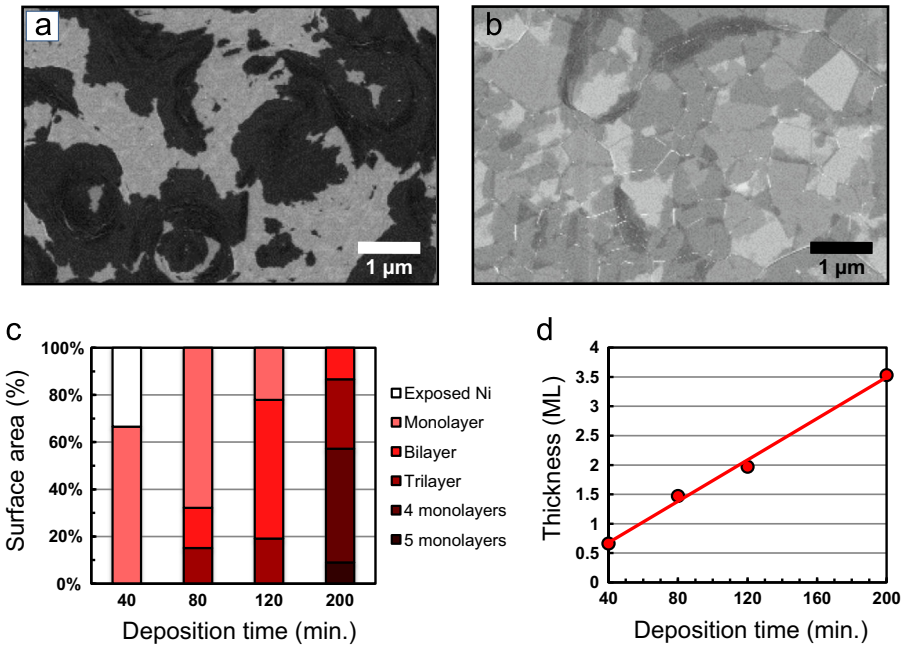

Fig. 4. SEM micrographs of graphene grown on Ni/MgO (111) for 40 min (a), and 200 min (b). The dark regions in (a) are graphene, while the lighter regions are exposed Ni, showing this film did not reach a full monolayer. The entire surface in (b) is covered in graphene, with the darker regions being thicker portions of the film. A complete monolayer of graphene forms prior to any multilayer formation (c), and the thickness disorder increases with deposition time. The average thickness of the graphene films scale well with deposition time (d).

for the dielectric substrates. The remaining carbon likely desorbs from the substrate surface prior to incorporation. In the case of the Ni/MgO (111) substrates, it may also dissolve into the metal. Because surface features have been shown to influence graphene growth, it is anticipated that further optimization of substrate surface will allow for increased thickness homogeneity [24,30,42].

4. Conclusions

The results presented here attest to the feasibility of employing MBE to controllably synthesize not only single-, but also few-layer thick graphene films on various templates. They also emphasize that more detailed investigations are still needed to completely elucidate the nucleation and growth mechanisms involved. It has been shown that state-of-the-art structural quality can be achieved for graphene grown on a metallic surface by MBE. For graphene layers prepared directly on insulators, a higher density of defects is verified. Nevertheless, the findings obtained for the latter case are particularly significant as they show that an epitaxial process takes place during MBE growth on these substrates [$6\sqrt{3}$-SiC (0001) and Al_2O_3 (0001)]. That strict epitaxy occurs on these substrates, which largely removes rotational disorder, means that the implementation of optimized synthesis conditions will enable the fabrication of large-area graphene films which possess a precise number of atomic layers, large domain sizes, and therefore offer excellent electronic properties.

Acknowledgments

The authors would like to thank Oliver Bierwagen for the critical reading of the manuscript, Claudia Herrmann, Michael Höricke, and Hans-Peter Schönherr for their valuable technical support. The authors thank the ESRF for providing beamtime during project SI-2449 and Roberto Nervo for his support during the experiment.

References

[1] K.S. Novoselov, A.K. Geim, S.V. Morozov, D. Jiang, Y. Zhang, S.V. Dubonos I.V. Grigorieva, A.A. Firsov, Science 306 (2004) 666.
[2] C. Berger, Z. Song, T. Li, X. Li, A.Y. Ogbazghi, R. Feng, Z. Dai, A.N. Marchenkov E.H. Conrad, P.N. First, W.A. de Heer, J. Phys. Chem. B 108 (2004) 19912.
[3] Y. Zhang, Y.-W. Tan, H.L. Stormer, P. Kim, Nature 438 (2005) 201.
[4] M.S. Fuhrer, C.N. Lau, A.H. MacDonald, MRS Bull. 35 (2010) 289.
[5] J.B. Oostinga, H.B. Heersche, X. Liu, A.F. Morpurgo, L.M.K. Vandersypen, Nat. Mater. 7 (2008) 151.
[6] C.H. Lui, Z. Li, K.F. Mak, E. Cappelluti, T. Heinz, Nat. Phys. 7 (2011) 944.
[7] Y. Zhang, T.-T. Tang, C. Girit, Z. Hao, M.C. Martin, A. Zettl, M.F. Crommie Y.R. Shen, F. Wang, Nature 459 (2009) 820.
[8] B.N. Szafranek, D. Schall, M. Otto, D. Neumaier, H. Kurz, Nano Lett. 11 (2011) 2640.
[9] K.S. Novoselov, V.I. Falko, L. Colombo, P.R. Gellert, M.G. Schwab, K. Kim, Nature 490 (2012) 192.
[10] K.V. Emtsev, A. Bostwick, K. Horn, J. Jobst, G.L. Kellogg, L. Ley, J.L. McChesney, T. Ohta, S.A. Reshanov, J. Röhrl, E. Rotenberg, A.K. Schmid, D. Waldmann H.B. Weber, T. Seyller, Nat. Mater. 8 (2009) 203.
[11] W.A. de Heer, C. Berger, M. Ruan, M. Sprinkle, X. Li, Y. Hu, B. Zhang, J. Hankinson, E. Conrad, Proc. Natl. Acad. Sci. 108 (2011) 16900.
[12] M.H. Oliveira Jr., T. Schumann, M. Ramsteiner, J.M.J. Lopes, H. Riechert, Appl. Phys. Lett. 99 (2011) 111901.
[13] X. Li, W. Cai, J. An, S. Kim, J. Nah, D. Yang, R. Piner, A. Velamakanni, I. Jung, E. Tutuc, S.K. Banerjee, L. Colombo, R.S. Ruoff, Science 324 (2009) 1312.
[14] S. Bae, H. Kim, Y. Lee, X. Xu, J.-S. Park, Y. Zheng, J. Balakrishnan, T. Lei1 H.R. Kim, Y.I. Song, Y.-J. Kim, K.S. Kim, B Ozyilmaz, J.-H. Ahn, B.H. Hong, S. Iijima, Nat. Nanotech. 5 (2010) 574.
[15] W.P. McCray, Nat. Nanotech. 2 (2007) 259.
[16] J. Hackley, D. Ali, J. DiPasquale, J.D. Demaree, C.J.K. Richardson, Appl. Phys. Lett. 95 (2009) 133114.
[17] F. Maeda, H. Hibino, Jpn. J. Appl. Phys. 49 (2010) 04DH13.
[18] U. Wurstbauer, T. Schiros, C. Jaye, A.S. Plaut, R. He, A. Rigosi, C. Gutiérrez, D. Fischer, L.N. Pfeiffer, A.N. Pasupathy, A. Pinczuk, J.M. Garcia, Carbon 50 (2012) 4822.
[19] E. Moreau, S. Godey, F.J. Ferrer, D. Vignaud, X. Wallart, J. Avila, M.C. Asensio, F. Bournel, J.-J. Gallet, Appl. Phys. Lett. 97 (2010) 241907.
[20] S.K. Jerng, J.H. Lee, D.S. Yu, Y.S. Kim, J. Ryou, S. Hong, C. Kim, S. Yoon, S.H. Chun, J. Phys. Chem. C 116 (2012) 7380.
[21] M.H. Oliveira Jr, T. Schumann, R. Gargallo, F. Fromm, T. Seyller, M. Ramsteiner, A. Trampert, L. Geelhaar, J.M.J. Lopes, H. Riechert, Carbon 56 (2013) 339.
[22] S. Wang, L.F. dos Santos, U. Wurstbauer, L. Wang, L.N. Pfeiffer, J. Hone J.M. Garcia, A. Pinczuk, Solid State Commun. 189 (2014) 15.
[23] J.M. Garcia, R. He, M.P. Jiang, J. Yan, A. Pinczuk, Y.M. Zuev, K.S. Kim, P. Kim, K. Baldwin, K.W. West, L.N. Pfeiffer, Solid State Commun. 150 (2010) 809.
[24] J.M. Wofford, M.H. Oliveira Jr., T. Schumann, B. Jenichen, M. Ramsteiner, U. Jahn, S. Fölsch, J.M.J. Lopes, H. Riechert, New J. Phys. 16 (2014) 093055.
[25] G. Lippert, J. Dabrowski, Y. Yamamoto, F. Herziger, J. Maultzsch, M.C. Lemme, W. Mehr, G. Lupina, Carbon 52 (2013) 40.
[26] P.W. Sutter, J.-I Flege, E.A. Sutter, Nat. Mater. 7 (2008) 406.
[27] E. Loginova, N.C. Bartelt, P.J. Feibelman, K.F. McCarty, New J. Phys. 10 (2008) 93026.
[28] E. Loginova, N.C. Bartelt, P.J. Feibelman, K.F. McCarty, New J. Phys. 11 (2009) 063046.
[29] J.M. Wofford, S. Nie, K.F. McCarty, N.C. Bartelt, O.D. Dubon, Nano Lett. 10 (2010) 4890.
[30] S. Nie, J.M. Wofford, N.C. Bartelt, O.D. Dubon, K.F. McCarty, Phys. Rev. B 84 (2011) 155425.
[31] J.M. Wofford, E. Starodub, A.L. Walter, S. Nie, A. Bostwick, N.C. Bartelt, K. Thürmer, E. Rotenberg, K.F McCarty, O.D. Dubon, New J. Phys. 14 (2012) 053008.
[32] T. Schumann, M. Dubslaff, M.H. Oliveira Jr., M. Hanke, F. Fromm, T. Seyller, L. Nemec, V. Blum, M. Scheffler, J.M.J. Lopes, H. Riechert, New J. Phys. 15 (2013) 123034.
[33] A.C. Ferrari, J. Meyer, V. Scardaci, C. Casiraghi, M. Lazzeri, F. Mauri, S. Piscanec, D. Jiang, K.S. Novoselov, S. Roth, A.K. Geim, Phys. Rev. Lett. 97 (2006) 187401.
[34] A.C. Ferrari, D.M. Basko, Nat. Nanotechnol. 8 (2013) 235.
[35] L.G. Cançado, A. Jorio, E.H. Martins Ferreira, F. Stavale, C.A. Achete, R.B. Capaz, M.V.O. Moutinho, A. Lombardo, T.S. Kulmala, A.C. Ferrari, Nano Lett. 11 (2011) 3190.
[36] S. Goler, C. Coletti, V. Piazza, P. Pingue, F. Colangelo, V. Pellegrini, K.V. Emtsev, S. Forti, U. Starke, F. Beltram, S. Heun, Carbon 51 (2013) 249.
[37] T. Schumann, M. Dubslaff, M.H. Oliveira Jr., M. Hanke, J.M.J. Lopes, H. Riechert, Phys. Rev. B 90 (2014) 041403(R).
[38] K.V. Emtsev, F. Speck, T. Seyller, L. Ley, J. Riley, Phys. Rev. B 77 (2008) 155303.
[39] H. Hattab, A.T. N'Diaye, D. Wall, C. Klein, G. Jnawali, J. Coraux, C. Busse, R. van Gastel, B. Poelsema, T. Michely, F.-J. Meyer zu Heringdorf, M. Horn-von Hoegen, Nano Lett. 12 (2012) 678.
[40] A. Koma, Thin Solid Films 216 (1992) 72.
[41] R. Addou, A. Dahal, P. Sutter, M. Batzill, Appl. Phys. Lett. 100 (2012) 021601.
[42] J. Dabrowski, G. Lippert, T. Schroeder, G. Lupina, Appl. Phys. Lett. 105 (2014) 191610.